

# Extracting mechanical work from a scalar field potential via dissipative structures

Mark Gibbons CEng MEI

Target Carbon Limited, 271 Coppice Road, Poynton, Stockport, Cheshire, SK12 1SP, United Kingdom

Email: [markgibbons@targetcarbon.co.uk](mailto:markgibbons@targetcarbon.co.uk)

## Abstract

Further thermodynamic investigations into the behaviour of a polar dielectric working fluid under non-equilibrium and negative pressure conditions are reported. The establishment of a long-range van der Waals interaction between clathrate hydrates and their former guest molecules is revisited. The dissipative nature of these inclusion compounds appears responsible for second-order phase changes that maintain a constant Hamiltonian function despite distinct changes in phase symmetry. A scalar field potential, as derived from the Lagrangian function, is deemed responsible for the flow of energy within the system. The inclusion compounds are embedded in a geometrically frustrated fluid lattice which together form a 'spin ice' material. The effective magnetic monopoles of the 'spin ice' appear to exchange energy with the long-range van der Waals interaction on a hyperbolic manifold to produce mechanical work. For expansion work, the exchange of energy continues up to a transition point where the auxiliary magnetic field is deemed reach zero potential. However, expansion work continues well beyond this transition point, driven by a gradient energy that now exceeds the expression of curvature on the hyperbolic manifold. Emergent geometry associated with vacuum energy is proposed as the most likely source for the missing energy contribution.

## Keywords

non-equilibrium system; low energy negative pressure system; inertial effects; geometrically frustrated lattice; hyperbolic curvature; scalar field potential; gradient energy; emergent geometry

## Introduction

Previous work examined non-additive and non-extensive interactions arising from a non-equilibrium, metastable system subjected to negative pressure conditions [1]. In these experiments, the system was held under constant-volume, ie. isochoric conditions, with a quasi-thermodynamic cycle performed across liquid and vapour phases. The structural inertia of dissipative, clathrate hydrate structures, sustained by a flow of negative entropy, was deemed to be responsible for the emergence of a long-range van der Waals (vdW) interaction able to perform phase-change work within a quasi-thermodynamic cycle. In reaching this conclusion, it was necessary to discard classical thermodynamic assumptions of a quasi-static and isolated system, although the system can still be described by the classical virial theorem [2].

The investigations reported here seek to extend the effectiveness of the long-range interaction to create mechanical work output in a kinetic system, ie. one performing variable-volume work. The results are presented in a number of charts obtained from recorded and calculated data. To develop plausible theories to describe the experimental results, it is necessary to re-visit our earlier approach to the fundamental thermodynamic relation and the non-additivity/ non-extensivity arising. The previous results describe a linear oscillator behaving as a self-gravitating system with a constant Hamiltonian function [1]. Examining the Lagrangian function of the latest variable-volume system, evidence for a scalar field interaction is presented through the existence of a gradient energy term.

Although the fluid formulation has been modified for the latest variable-volume experiments, it appears anomalous that the quasi-thermodynamic cycle now proceeds entirely within the liquid phase. Large disparities arise between the fluid density and the swept volume of the system leading to non-extensivity. The curvature of the system is investigated as the cause of this disparity and how it relates to the structural inertia of the

dissipative, clathrate structures. For the constant Hamiltonian function, a simplified Bernoulli expression is employed to derive the velocity of the incompressible fluid as a proxy for its hyperbolic curvature.

The tetrahedral molecular structure of the working fluid resembles a corner-sharing pyrochlore lattice [3,4]. Using this comparison, the working fluid behaviour is treated as a geometrically frustrated system capable of producing novel magnetic effects. Such 'spin ice' materials represent a source of effective magnetic monopoles [5].

The modern approach to classifying phase transitions is established with two broad categories. First-order transitions incorporate isobaric, latent heat transfers. Second-order transitions do not involve latent heat behaviour and are characterised by a continuous change in specific volume and entropy. Second-order phase transitions can be associated with an emergence of magnetism, superconductivity, superfluidity and orientational order [6].

The investigations go on to explore how inertial effects can arise in systems with magnetic charge and explore whether the resulting interactions provide a credible mechanism for the conversion of a long-range vdW potential into mechanical work. This work term can be related to the gradient energy term of the Lagrangian, issuing from a scalar field potential. However, the gradient energy term cannot be fully accounted for in terms of hyperbolic curvature at all times and an additional, intermittent source needs to be accounted for.

The solution should produce energy conservation for the kinetic cycles performed experimentally. To achieve such symmetry, potential solutions involving broken gauge invariance [7], dual superconductivity [8] and the Meissner effect [8] are speculated.

### Methods and materials

The original objective for this research was to reduce compression-stage losses associated with thermodynamic cycles. Isochoric thermo-compression [9] of polar dielectric fluids at temperatures below 100°C was selected as a suitable area of investigation to reduce the mechanical compression penalties associated with irreversible thermodynamic cycles.

Initial modelling with the NIST REFPROP program/ database [10] together with the experimental investigation targeted thermal instabilities arising from strong interactions between attractive and repulsive molecular forces as a source of thermo-compression energy. Through empirical observation and results, it became possible to establish a repeatable quasi-thermodynamic cycle through the controlled application of heat flux. With the application of heating and cooling only (ie. no external work input) an ideal, isochoric cycle has been established. The refined process arrived at is described in previous work [1].

The original apparatus is modified such that the 5 litre pressure vessel is here replaced with a 0.5 litre piston accumulator/ expander, as described in **Fig. 1** below:

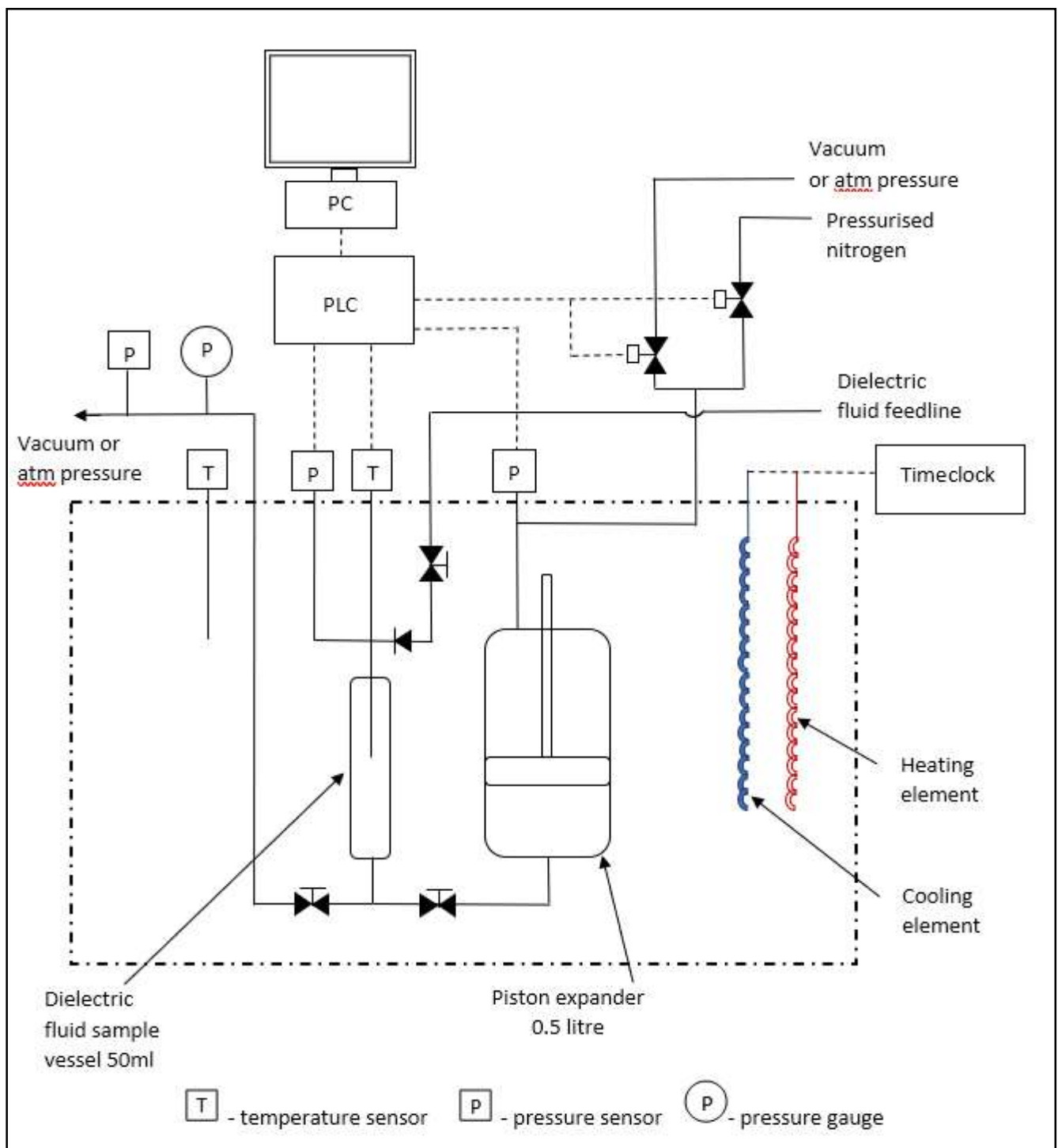


Fig. 1: Schematic arrangement of the experimental apparatus

The current investigations also involve a polar dielectric working fluid of multi-component formulation, consisting of water and methane within an inhibitor solvent engineered such that the equilibrium between attractive and repulsive molecular forces is readily destabilised when the fluid is subjected to variable pressure. The nature and purpose of the clathrate inhibitor has previously been described in detail by Perrin *et al* [11]. Our latest inhibitor formulation is designed to maximise the mechanical expansion work of a quasi-thermodynamic cycle at relatively low-temperatures (ie. below 20°C). Changes in the polar dielectric properties are pressure-induced with a view to creating a quasi-thermodynamic cycle through non-equilibrium, irreversible expansion and contraction.

A negative pressure fluid is created by means broadly similar to the Berthelot-method [12]. The working fluid, as specially formulated for this application, fills a previously evacuated stainless-steel sample vessel (50ml), as Fig. 1 above. The sample vessel is completely immersed in a relatively large heat bath (70 litres) where the temperature of the bath is controlled with an electric element and a refrigeration dip cooler.

Once the desired temperature is obtained, the sample is released into the fluid-side of the 0.5 litre retracted piston expander which moves the piston vertically upwards to the fully-extended position. The gas-side of the piston is open to atmospheric pressure during this extension. The gas-side outlet is then isolated from atmospheric pressure. Through the application of pressurised nitrogen gas, the piston is returned to its fully-retracted position and the valve between the sample vessel and the piston expander closed such that the effective sample is now only 5ml, approx. At this point the pressurised nitrogen is released to atmosphere and the working fluid once again allowed to expand to deliver mechanical work to the piston.

The extent of the piston movement is recorded to determine the  $P$ - $V$  work input and output resulting. This cyclic process can be repeated many times without any apparent degradation in the  $P$ - $V$  work output or the speed of operation. The temperature and pressure of the working fluid are measured at five-second intervals with sensors that are in direct contact with the fluid and recorded by a PLC/ PC monitoring system.

## Results

Returning initially to the original isochoric results, heat input and work output from the two-phase medium can be determined from **Fig. 2** and **Fig. 3** below using the approach described earlier [1]:

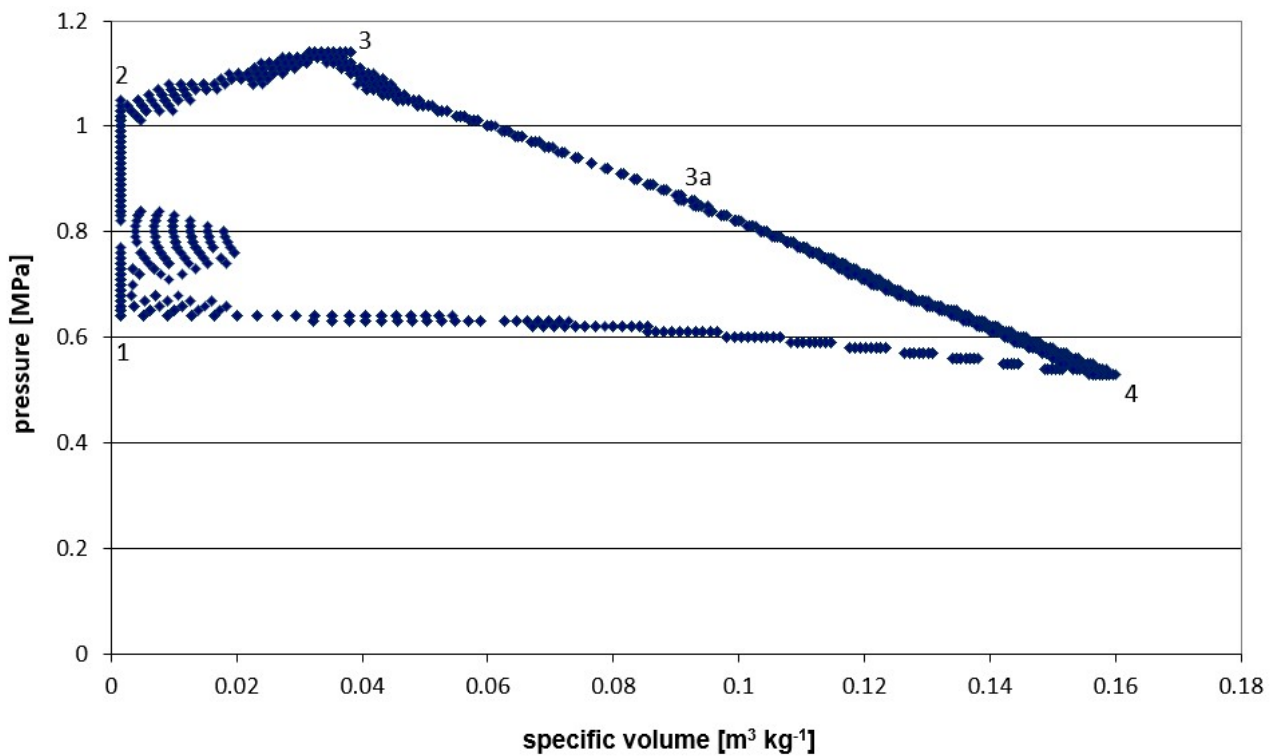


Fig. 2: Isochoric phase-change work can be determined from the  $P$ - $v$  chart

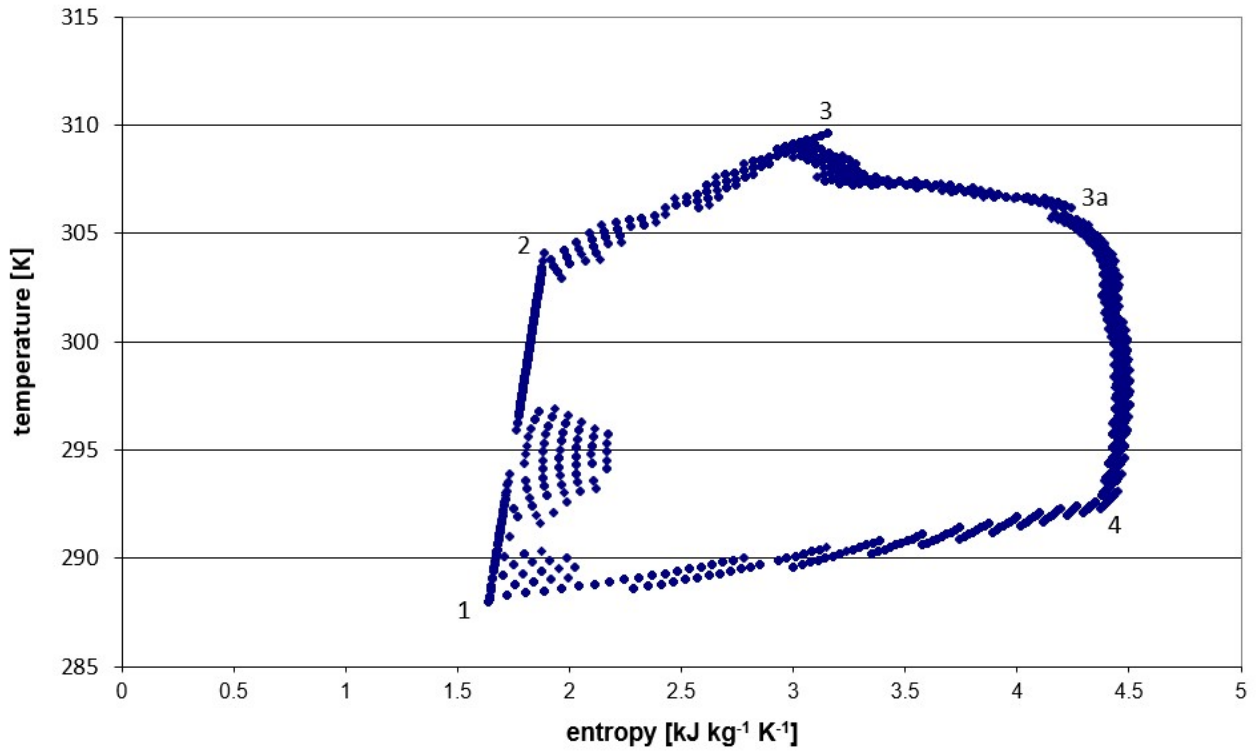


Fig. 3: Isochoric heat input can be determined from the  $T$ - $s$  chart

The variable-volume results from the latest piston-expander apparatus are now presented and described. Direct temperature and pressure measurements for a manually controlled sequence of 10-cycles produce the profiles in Fig. 4. The heat bath temperature on this occasion is  $-2.5^{\circ}\text{C}$ , approx. Stage 1-2 represents compression of the working fluid from an externally applied nitrogen gas pressure. Stage 3-4 represents expansion of the working fluid as the nitrogen pressure is removed:

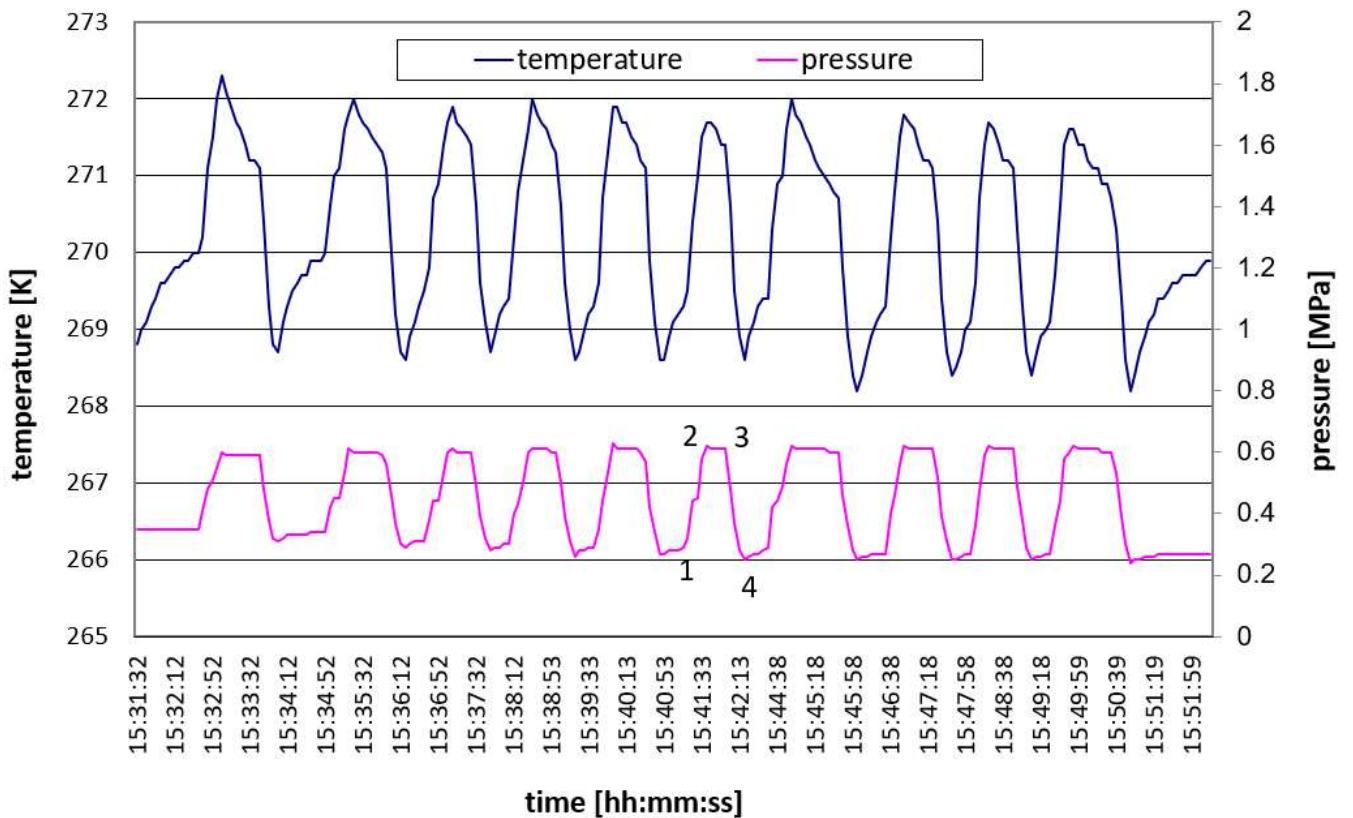


Fig. 4: Temperature and pressure profiles for a sequence of 10-cycles

Calculated thermodynamic properties for Points 1-4 are included in **Table 1** below:

Table 1: Recorded and calculated thermodynamic properties of a typical piston expander cycle

	Temperature $T$ (K)	Pressure $P$ (MPa)	specific volume $v$ (m <sup>3</sup> /kg)
Point 1	269.3	0.29	0.0015
Point 2	271.7	0.62	0.0015
Point 3	271.4	0.61	0.0015
Point 4	268.6	0.25	0.0015

	internal energy $u$ (kJ/kg)	entropy $s$ (kJ/kg-K)	Volume $V$ (m <sup>3</sup> )
Point 1	-209.3	0.79	0.000505
Point 2	-200.6	0.83	0.000005
Point 3	-201.7	0.82	0.000005
Point 4	-211.9	0.78	0.000505

	$\Delta T$ - $s$ heat (kJ/kg)	$\Delta P$ - $v$ work (kJ/kg)	$\Delta P$ - $V$ work (kJ/kg)
Compress 1-2	1.93	0.0015	642.9
Expand 3-4	-2.23	-0.0015	-568.6

At just over 1%, it is clear that the ideal Carnot efficiency ( $1 - T_c/T_h$ ) cannot adequately describe the non-equilibrium system. In addition, the actual thermodynamic efficiencies of both compression and expansion processes ( $\Delta P$ - $v/\Delta T$ - $s$ ) are significantly lower, at less than 0.1%

As with the isochoric results [1], the variable-volume experiments produce a distortion of the short-range energy interactions through the presence of a non-concave entropy function of internal energy, as Fig. 5:

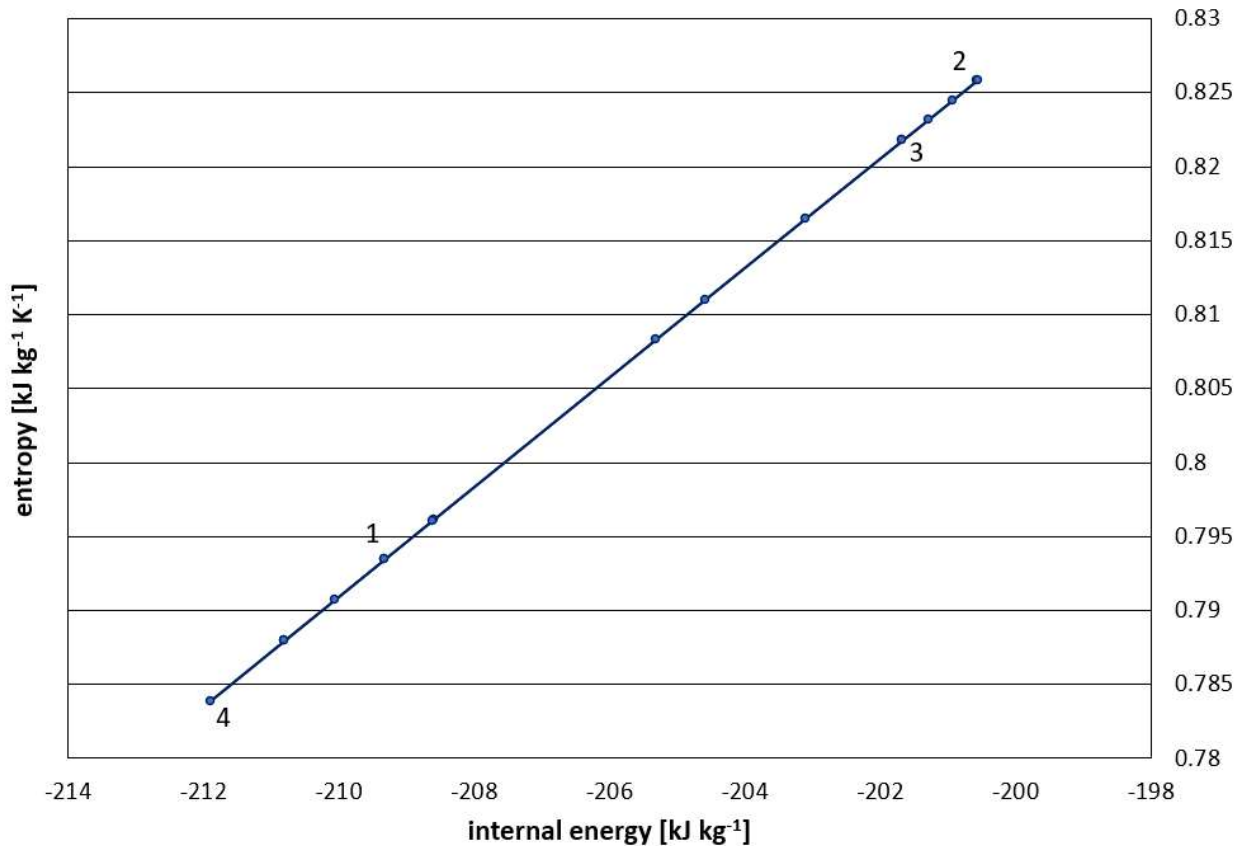
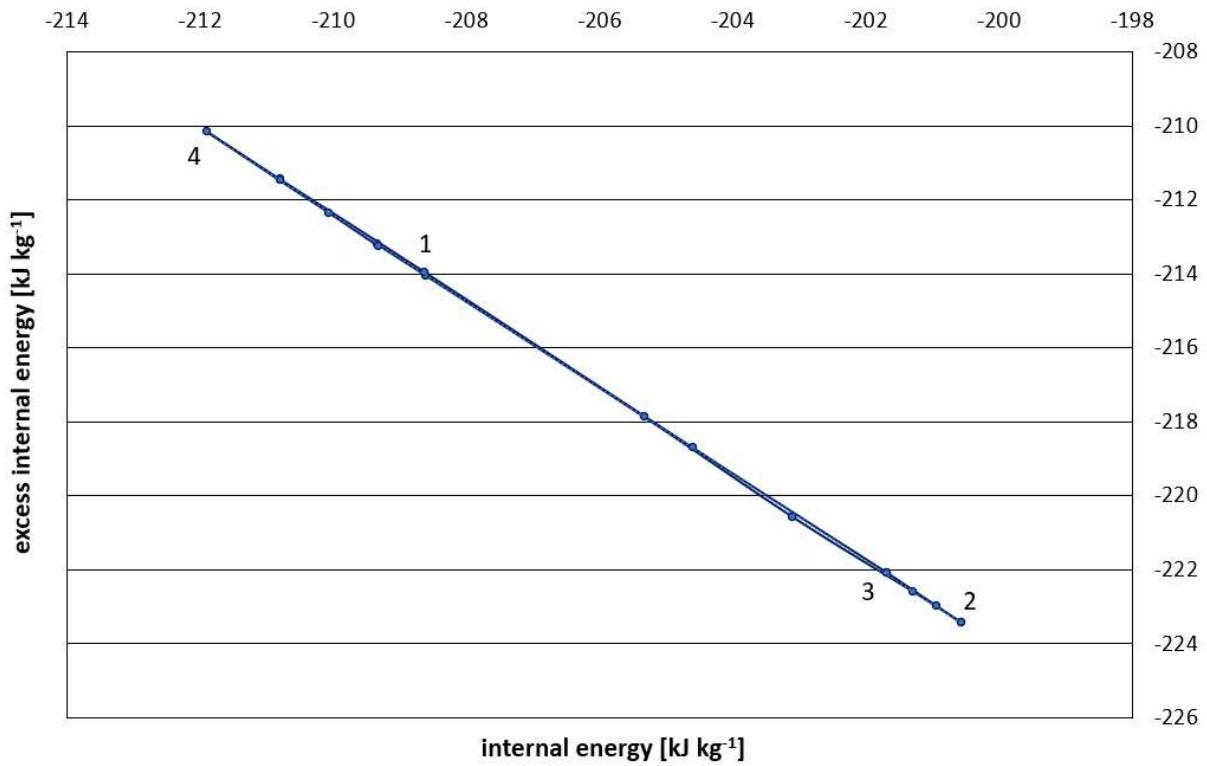


Fig.5: Affine (non-concave) entropy function revealing a distortion of the short-range interaction

Relative, negative values of internal energy indicate a low energy system, resulting from negative pressure. Since enthalpy of the system is dominated by internal energy, a linear enthalpy-entropy compensation effect is also present [13].

A further correspondence with the original isochoric results [1] arises from the excess negative internal energy; seen as a disparity between the internal energy and the fundamental thermodynamic relation for the non-equilibrium system, as **Fig. 6**:



**Fig. 6: Excess internal energy resulting from excess thermodynamic potentials**

When proceeding through a cycle, the calculated density (or  $1/v$ ) remains almost constant such that it is not possible to generate work output from a first-order phase transition. However, **Fig. 7** below reveals similar values for work input and work output:

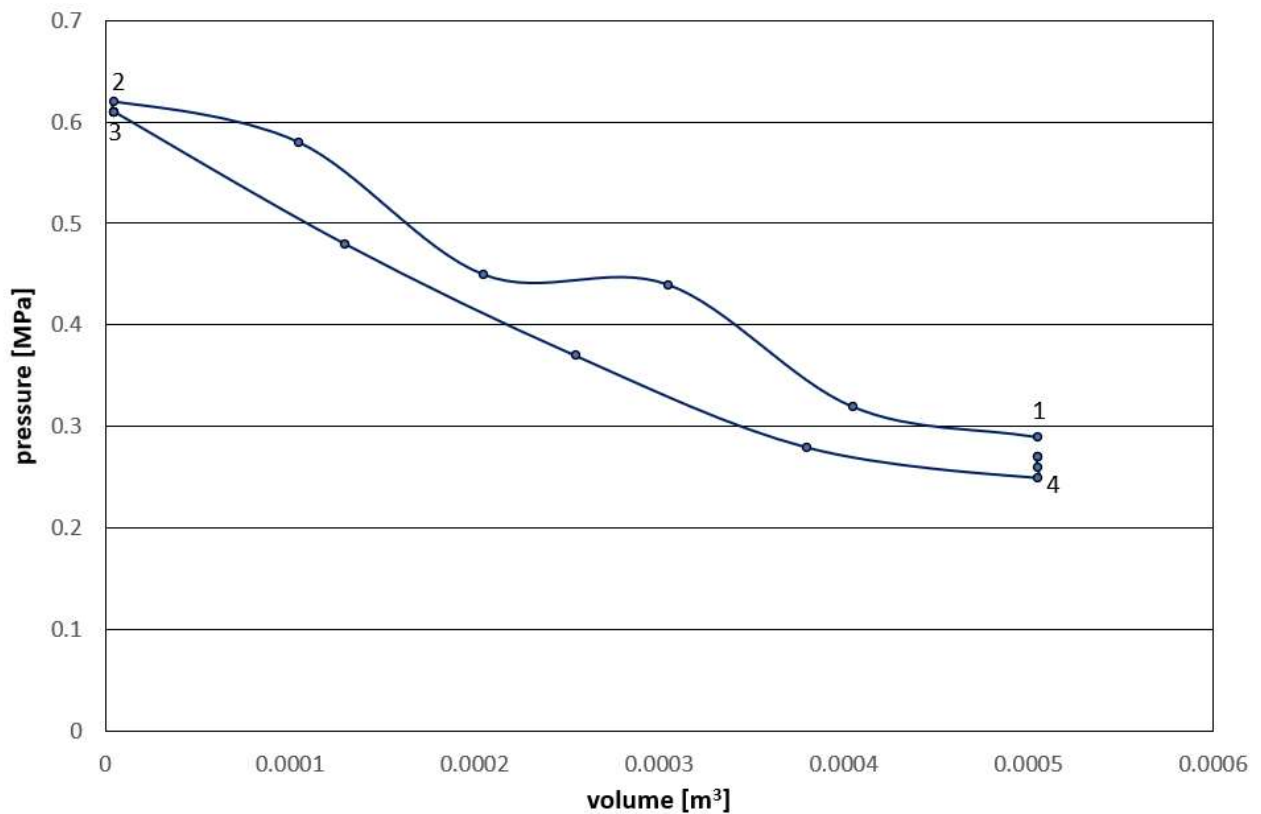


Fig. 7:  $P$ - $V$  work input and  $P$ - $V$  work output can be determined

The disparity between  $P$ - $v$  and  $P$ - $V$  can be considered in terms of external fluid curvature, calculated through application of a simple Bernoulli expression for an incompressible flow, as shown in **Fig. 8**:

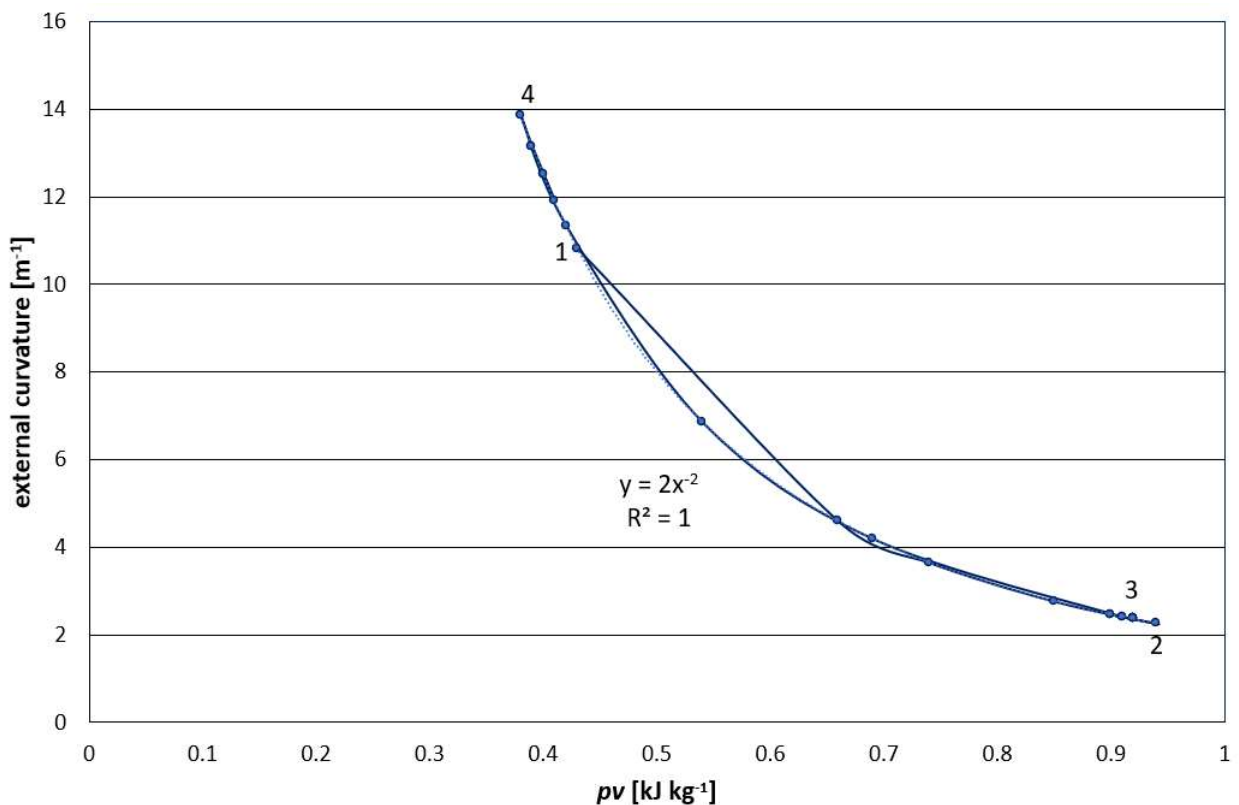


Fig. 8: External curvature from a simple Bernoulli equation for an incompressible flow

The inertia of the dissipative system is then considered in terms of the standard formulation for a cylinder,  $\frac{1}{2} mr^2$ , where an almost exact 1:1 mapping is established in **Fig. 9**:

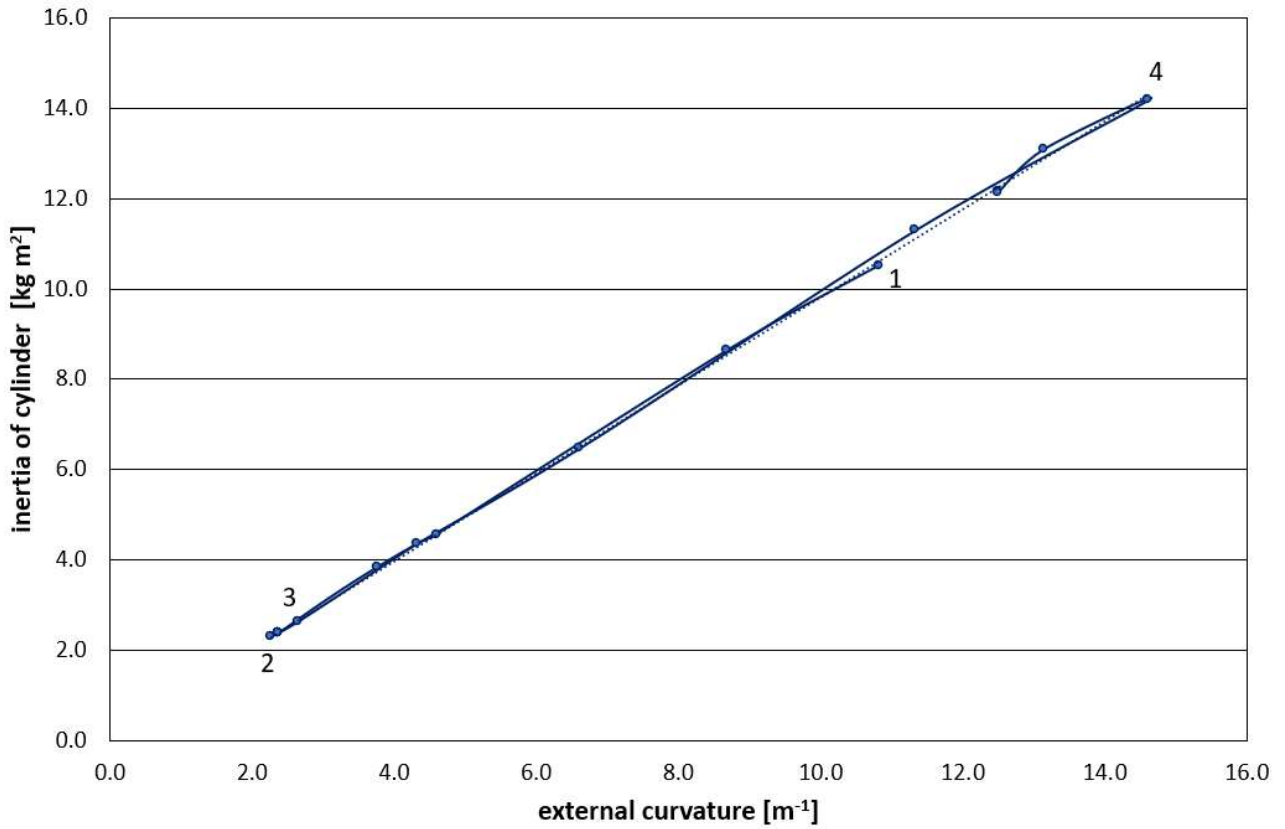


Fig. 9: Mapping of fluid inertia with external curvature

Where  $P$ - $V$  work is treated as the Lagrangian of the system then a gradient energy term, and hence a scalar field potential ( $\nabla\Phi$ ), arises. Evidence for a second-order phase transition is then revealed in **Fig. 10** since  $\nabla\Phi$  is a second order derivative with respect to the integrated  $P$ - $V$  work [6]. The transition occurs at TP1 whilst the return transition occurs at TP2:

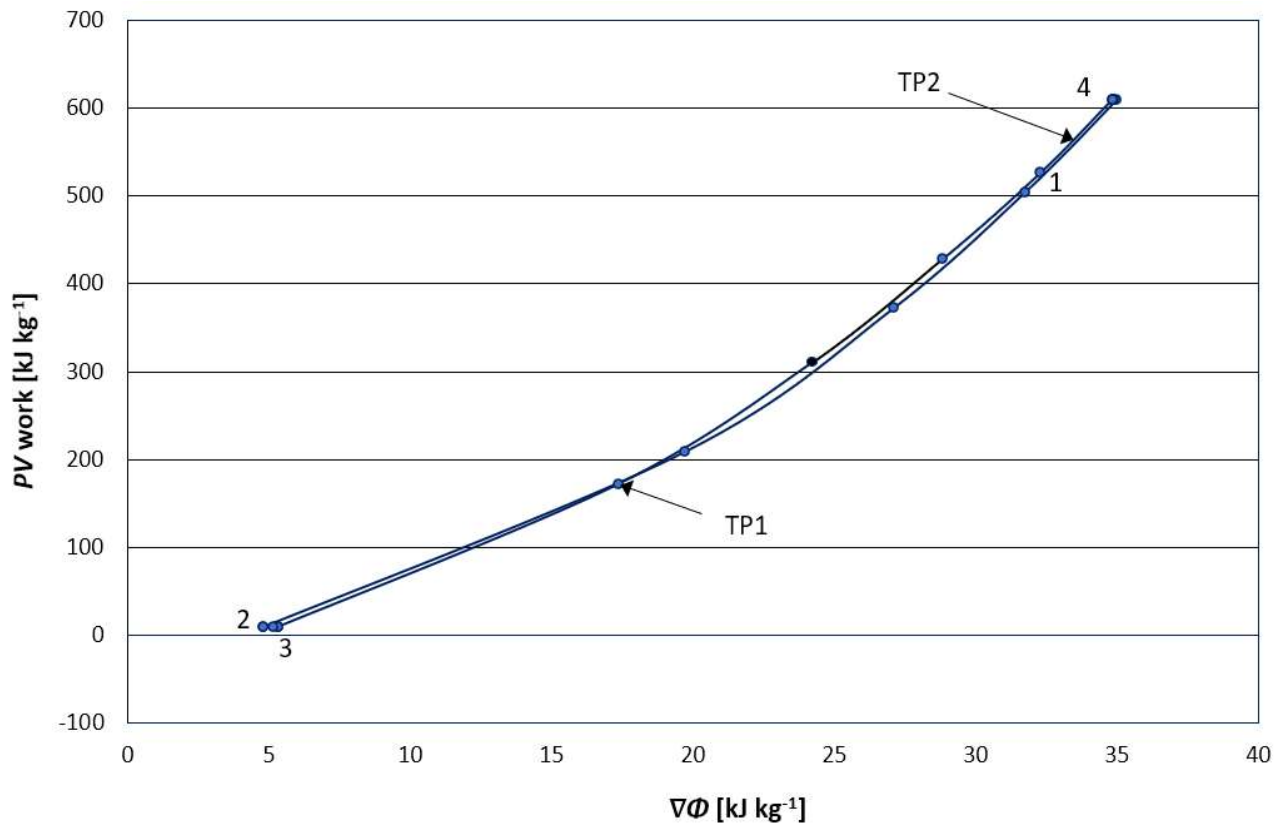


Fig. 10: Evidence for a scalar field potential ( $\nabla\Phi$ ) with second-order phase transition between TP1 and TP2

## Analysis & discussion

It is necessary to return initially to the fundamental thermodynamic relation, expressed as:

$$dU = Tds - Pdv + \sum_i \mu_i dn_i \quad (1)$$

where  $U$  is internal energy,  $T$  is temperature,  $P$  is pressure exerted on the boundary of the system,  $v$  is specific volume,  $s$  is specific entropy and

$$\sum_i \mu_i dn_i$$

is the specific chemical potential (Gibbs Energy) associated with bond formation or particle creation.

Under the isochoric condition, it was assumed that  $dn_i$  remained constant throughout the phase-change processes [1]. It was also suggested that the excess potential energy should be considered as a 'replica energy' term ( $\mathcal{E}$ ), since the potential appears to derive from statistical replicas of the system that differ only in phase or bond formation, ie. with respect to configuration and velocity [14]. However, most of the phase-changes involved in the cycle occurred under non-equilibrium conditions.

In seeking to maintain the universality of the fundamental thermodynamic relation for non-equilibrium situations, it is also necessary to consider  $\mu_i dn_i$  in terms of particle creation. For a phase-change process the following expression can be considered:

$$dU = (u_g - u_f)dm_{fg}$$

or

$$dU = d(m_g u_g + m_f u_f) \quad (2)$$

where:

$dm_{fg}$  is the mass transferred from liquid to vapour

$u_g$  is the specific internal energy of the saturated vapour,

$m_g$  is the mass of vapour,

$u_f$  is the specific internal energy of the saturated liquid, and

$m_f$  is the mass of liquid.

Masses are relative and derived from the liquid and vapour specific density values, as calculated by REFPROP and presented for the isochoric cycle in **Table 2**:

Table 2: Mass transfer in a 2-phase medium

	1	2	1 - 2	
	<b><i>U</i> from density/mass (kJ/kg)</b>	<b><i>U</i> from REFPROP (kJ/kg)</b>	<b>Difference in <i>U</i> (kJ/kg)</b>	<b><math>\Sigma</math> Difference or shortfall (kJ/kg)</b>
<b>Stage 1-2</b>	74	74	0	0
<b>Stage 2-3</b>	1075	348	727	727
<b>Stage 3-3a</b>	31	279	-248	479
<b>Stage 3a-4</b>	-9	1	-10	469
<b>Stage 4-1</b>	-1171	-702	-469	0

The following comparison of internal energy values can be made in Table 3:

Table 3: Comparison of mass transfer calculations

	1	2	1 - 2
	<b><i>u</i> from density/mass (kJ/kg)</b>	<b><i>u</i> from REFPROP (kJ/kg)</b>	<b>Difference in <i>u</i> (kJ/kg)</b>
<b>Point 1</b>	338	338	0
<b>Point 2</b>	412	412	0
<b>Point 3</b>	1487	760	727
<b>Point 3a</b>	1518	1039	479
<b>Point 4</b>	1510	1040	470

On the basis of mass transferred from liquid to vapour ( $dm_{fg}$ ), the internal energy at Point 3 is expected to be 1487 kJ kg<sup>-1</sup> versus an actual of 760 kJ kg<sup>-1</sup> calculated by REFPROP, ie. internal energy would be 96% higher on this basis. Since mass is determined by inertia, and the structural inertia of the guest-free clathrates has previously been observed [1], the discrepancy in internal energy of the cycle between Point 3 and Point 1 can now be explained by the energy-absorbing behaviour of the dissipative system, ie. its complex integrity is maintained by a flow of negative entropy. Such dissipative systems transform to more complex ones through higher degrees of organisation in response to externally induced sources of entropy [15].

For the latest variable-volume results, there is no associated vapour phase and the cycle proceeds under almost constant fluid density. However, it is still possible to detect inertial and negative entropy effects contained entirely within the liquid phase. This issue is explored further below.

The sequence of events depicted in **Fig. 4** is described by a typical cycle proceeding through Points 1-4:

Stage 1-2: apply pressurised nitrogen to the extended piston expander – piston retracts

Stage 2-3: pause – fluid temperature returning to equilibrium with heat bath

Stage 3-4: release nitrogen charge from the retracted piston expander – piston extends

Stage 4-1: pause – fluid temperature returning to equilibrium with heat bath

All stages are manually controlled which produces some minor differences between the cycle profiles.

The results in **Table 1** reveal a broken symmetry between  $P$ - $v$  work and  $P$ - $V$  work, ie. a system described by isolated and quasi-static assumptions does not result in energy conservation. To restore energy conservation, it is necessary to treat the system as open and non-equilibrium, where such conditions can produce non-thermodynamic work.

In the original isochoric results, the creation of a long-range vdW interaction between clathrate hydrates and their former guests was proposed [1]. This is described in **Fig. 11** and **Fig. 12** below:

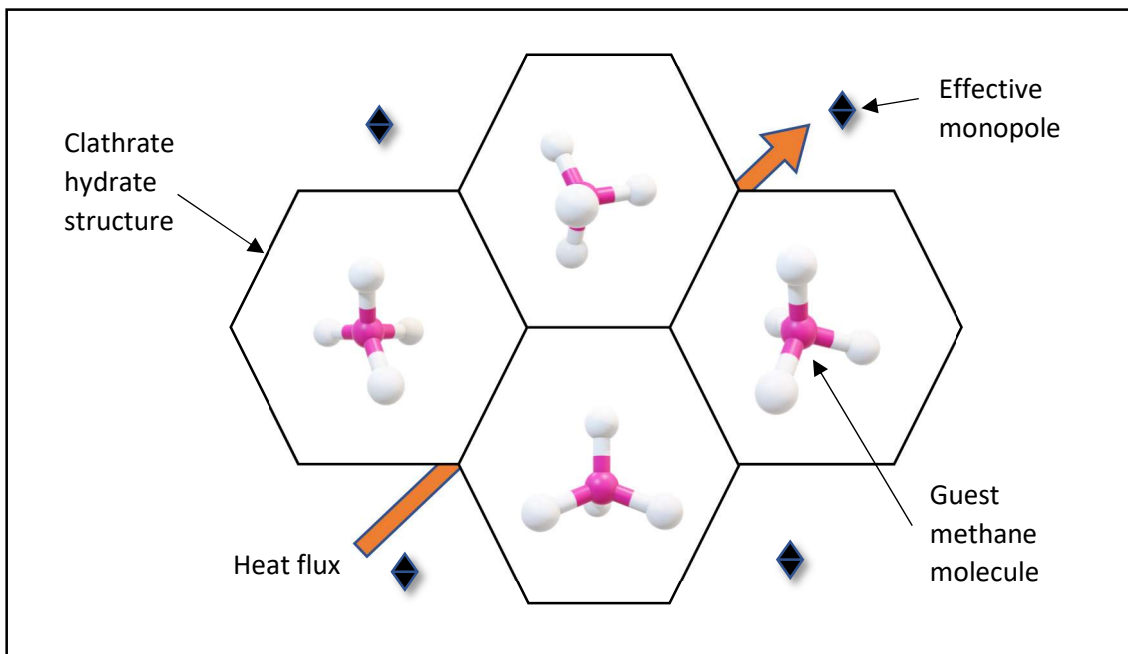


Fig. 11: Schematic of clathrate hydrate structure hosting methane molecules

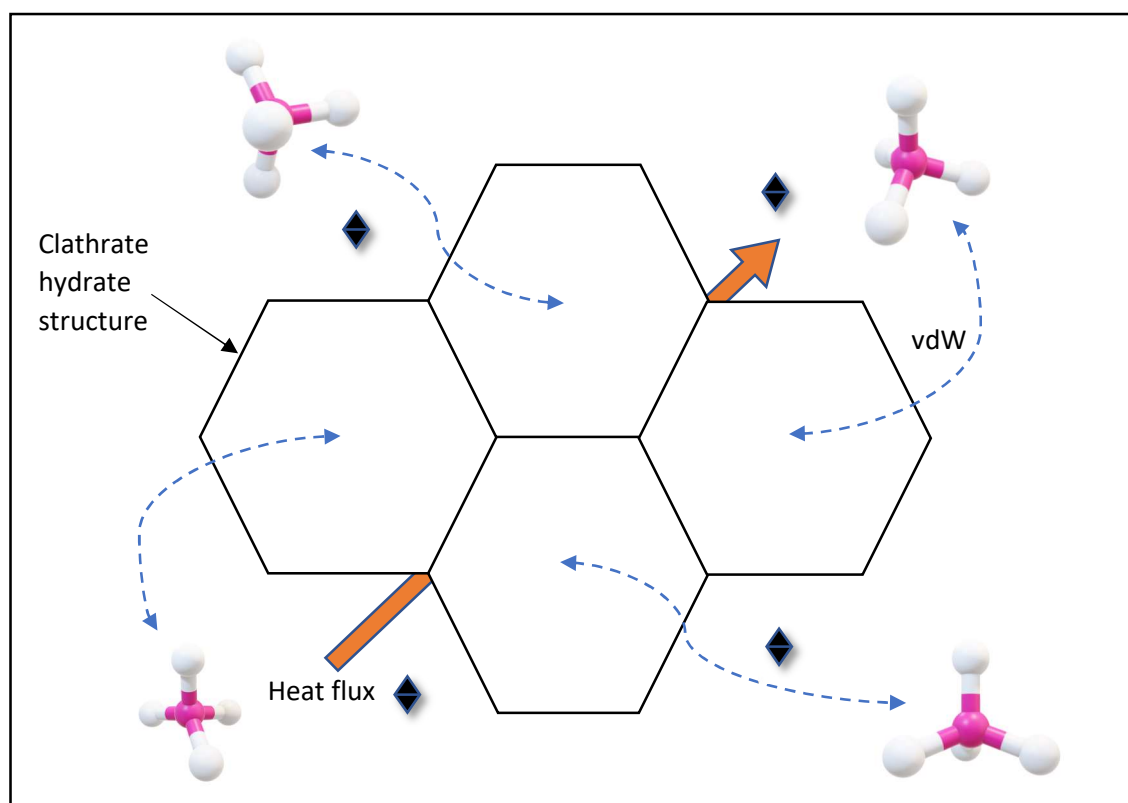


Fig. 12: Schematic of guest-free clathrate hydrate structure

A similar mechanism is again proposed for the large disparity between  $P$ - $v$  work and  $P$ - $V$  work in the variable-volume results. Here the disappearance of the long-range vdW interaction appears to be associated with growth of effective monopoles on the tetrahedral lattice. From the initial condition in **Fig. 12** the system now enters a state that is even further from equilibrium. This is shown schematically in **Fig. 13** below:

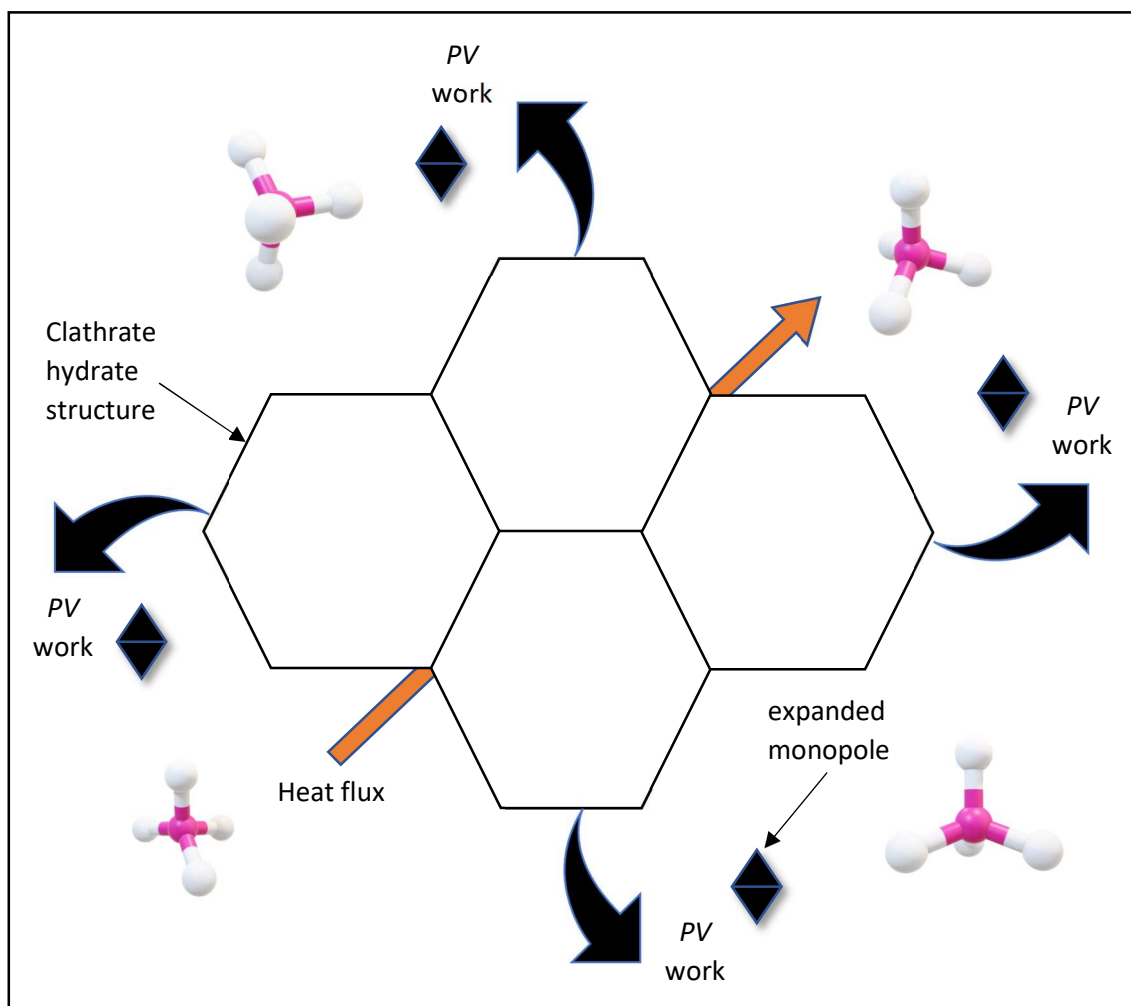


Fig. 13: Schematic of vdW interactions transmuted into  $P$ - $V$  expansion work

The creation of a dielectric solvent with disrupted, short-range electrostatic screening has been previously described [1]. This distortion of the short-range interaction is evident from the non-concave entropy function of internal energy such that a long-range vdW interaction with a  $-1/r$  relationship emerges. The linear profile of this non-concave entropy function also underpins an enthalpy-entropy compensation effect, interpreted as the organizational behaviour of the supramolecular chemistry [13].

Under the latest variable-volume conditions, **Fig. 5** is again consistent with the presence of a ‘magnetolyte’ in which weakly dissociated ions of water are correlated through hydrogen-bonded chains [16] such that clathrate hydrates subjected to negative pressure exhibit organizational behaviour in response to external thermodynamic inputs. **Fig. 6** confirms the dissipative nature of these complex cage structures through the mirroring of internal energy with excess negative energy potential that clearly describes a linear oscillator with constant Hamiltonian.

The large disparity between  $P$ - $v$  and  $P$ - $V$  is a feature of non-extensivity generated by the structural inertia of dissipative clathrate hydrate structures and sustained by a flow of entropy. This non-equilibrium condition manifests as hyperbolic, or negative, curvature when applying a simplified Bernoulli expression to the result in **Fig. 8** above:

$$\frac{V^2}{2} + \frac{P}{\rho} = \text{kinetic energy} + \text{potential energy} = \text{constant } E \quad (3)$$

where velocity  $V$  is taken as a proxy for relative curvature,  $P$  is the fluid pressure,  $\rho$  is the fluid density, and  $E$  is the total energy of the system.

For the linear oscillator of constant  $E$ ,  $P/\eta$  (or  $Pv$ ) is inversely proportional to kinetic energy. The internal curvature can be expressed as:

$$V = \sqrt{\frac{2}{Pv}}$$

The inverse gives the external curvature:

$$V = \frac{2}{(Pv)^2} \quad (4)$$

The inertial reaction of the dissipative fluid is now considered. The inertia associated with the fluid contained by the expansion cylinder can be described by the standard formulation:

$$I = \frac{1}{2}mr^2 \quad \text{or} \quad I = \frac{1}{2}r^2 \quad (5)$$

where specific properties are employed, eg.  $\text{kJ kg}^{-1}$ , and  $r$  is the cylinder radius. Equating inertia with relative curvature gives:

$$r = \frac{2}{Pv} \quad (6)$$

from which the values of hyperbolic circumference ( $2\pi \sinh(r)$ ) can be compared to Euclidean circumference ( $2\pi r$ ):

Table 4: Hyperbolic vs. Euclidean curvature

	1	2	1÷2
	<b>hyperbolic circumference <math>2\pi \sinh(r)</math></b>	<b>Euclidean circumference <math>2\pi r</math></b>	<b>ratio</b>
<b>Point 1</b>	329	29	11:1
<b>Point 2</b>	26	13	2:1
<b>Point 3</b>	27	14	2:1
<b>Point 4</b>	699	34	20:1

This analysis suggests that non-additivity and non-extensivity naturally arise from the structural inertia/hyperbolic manifold of the supramolecular fluid, able to sustain constant total energy  $E$  through complex reorganisation of clathrate hydrates and other molecular components. Despite this fluidity in reorganisation, ie. incompressible but having relatively non-viscous properties, the system still exhibits behaviour consistent with that of a tightly-bound lattice, ie. a tetrahedral molecular structure resembling a corner-sharing pyrochlore lattice [3,4]. Employing such a model, the working fluid behaviour is interpreted as a geometrically frustrated system producing novel magnetic effects. Such 'spin ice' materials are known to be a source of effective magnetic monopoles [5].

The previous isochoric experiments revealed a self-gravitating system, described in statistical mechanical terms by a non-equivalence of ensembles [1]. The latest variable-volume experiments are self-expanding such that the metastable system sustains a local minimum of energy by maximising inertial reaction and hyperbolic curvature. Again, the system represents an analogue of the false vacuum with a 'sombbrero potential'  $\nabla\Phi$ , that is in turn a function of a complex scalar field  $\Phi$  [17], as **Fig. 14** below:

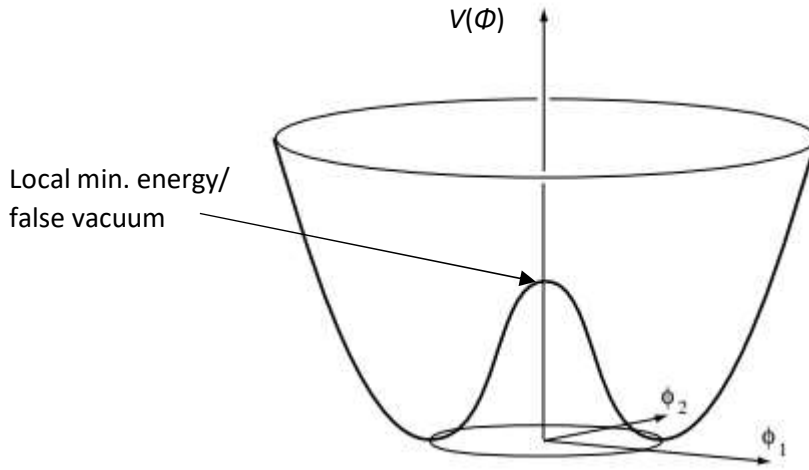


Fig. 14: The metastable, local minimum of energy in a sombrero potential

The high level of degeneracy required to stabilise this local minimum of energy [18] is confirmed by minimal deviations in Gibbs free energy across the complete cycle. Dissipative structures within the working fluid, sustained by a flow of negative entropy, impart a high level of stability to the metastable phase.

The system is now analysed in terms of a Lagrangian function whereby  $P$ - $V$  work is taken to conform to the principle of least action. Terms accounting for the kinetic, potential and interaction energies of the system are arranged to reveal a gradient energy term:

$$\frac{1}{2}(\nabla\Phi)^2 = i - i_{excess} - PV_{work} \quad (7)$$

where  $\frac{1}{2}(\nabla\Phi)^2$  is the gradient energy,  $i$  is internal energy, and  $i_{excess}$  is excess internal energy. The calculated data are included in Table 5 below:

Table 5:  $P$ - $V$  work expressed as a scalar potential

	$P$ - $V$ work [kJ kg <sup>-1</sup> ]	Gradient energy $\frac{1}{2}(\nabla\Phi)^2$ [kJ kg <sup>-1</sup> ]	Scalar potential $\nabla\Phi$ [kJ kg <sup>-1</sup> ]
<b>Point 1</b>	652	-648	51
<b>Point 2</b>	9	14	-8
<b>Point 3</b>	8	12	-7
<b>Point 4</b>	577	-579	48

	$\Delta P$ - $V$ work [kJ kg <sup>-1</sup> ]	$\Delta\frac{1}{2}(\nabla\Phi)^2$ [kJ kg <sup>-1</sup> ]	$\Delta\nabla\Phi$ [kJ kg <sup>-1</sup> ]
<b>Compress 1-2</b>	-643	662	-58
<b>Expand 3-4</b>	569	-591	55

$\nabla\Phi$  then corresponds to a scalar field potential. This is compared to  $P$ - $V_{work}$  in Fig. 10 from which the characteristic profile of a second-order phase transition is revealed [6]. The conditions under which such a transition might take place and the nature of any emergent properties will now be considered.

It seems reasonable that any theory attempting to describe the  $P$ - $V$  work recorded experimentally must propose a mechanism by which the gradient energy of a scalar field potential can enable mechanical work in the condensed matter system. How is it possible for a long-range vdW interaction between clathrates hydrates and their former guest molecules to manifest in forces that generate work? Earlier experiments revealed how a dielectric solvent under negative pressure could effectively neutralise all short-range interactions such that a 'clean'  $1/vx$  vdW interaction emerges [1]. Such long-range interactions are responsible for non-additive thermodynamic potentials and non-extensive system behaviour. During the expansion process, the scalar field potential increases as internal

energy decreases. Since this scalar field underpins a relatively large and negative gradient energy term, a repulsive force responsible for mechanical work is established.

A different phase exists between the scalar field value of  $17 \text{ kJ kg}^{-1}$  and  $34 \text{ kJ kg}^{-1}$ , approx. This corresponds to regions where the modulus value of the gradient energy exceeds that of the hyperbolic circumference. These parameters are compared within a geometric unit system over two cycles in **Fig. 11**. The pause intervals (Stages 2-3 and 4-1) are removed to improve clarity:

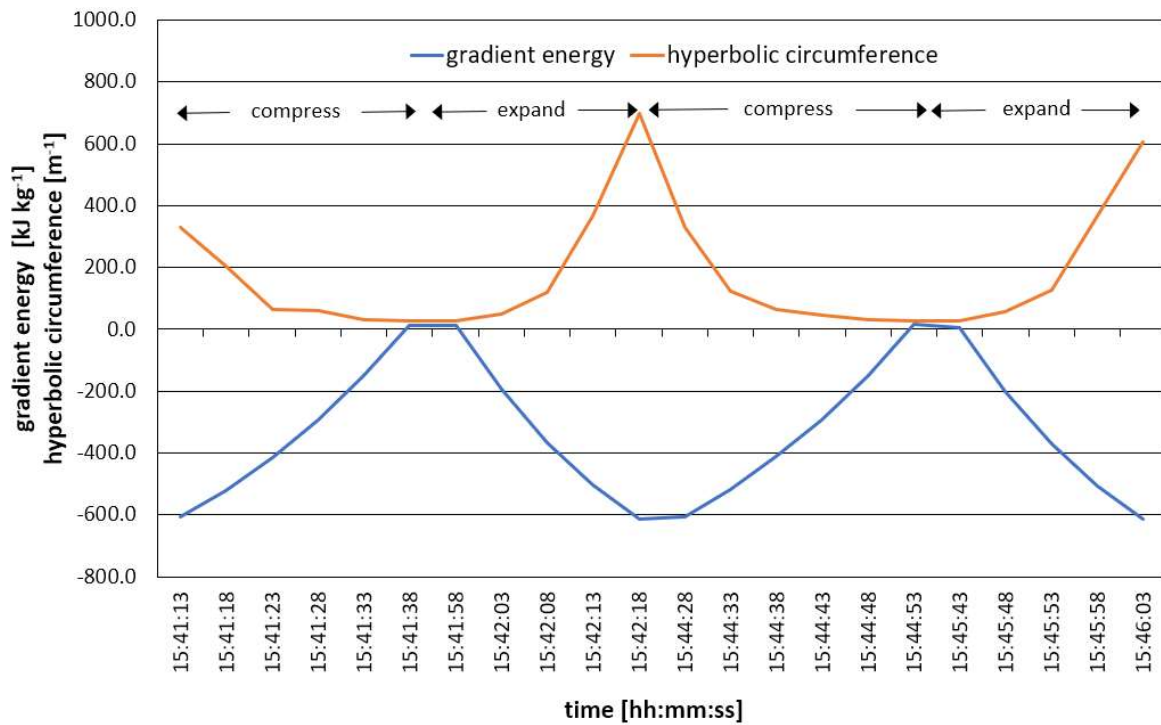


**Fig. 11. Comparison of gradient energy with hyperbolic circumference**

The working fluid enters a new phase for the shaded areas below the  $f(x) = 0$  axis in **Fig. 11**:

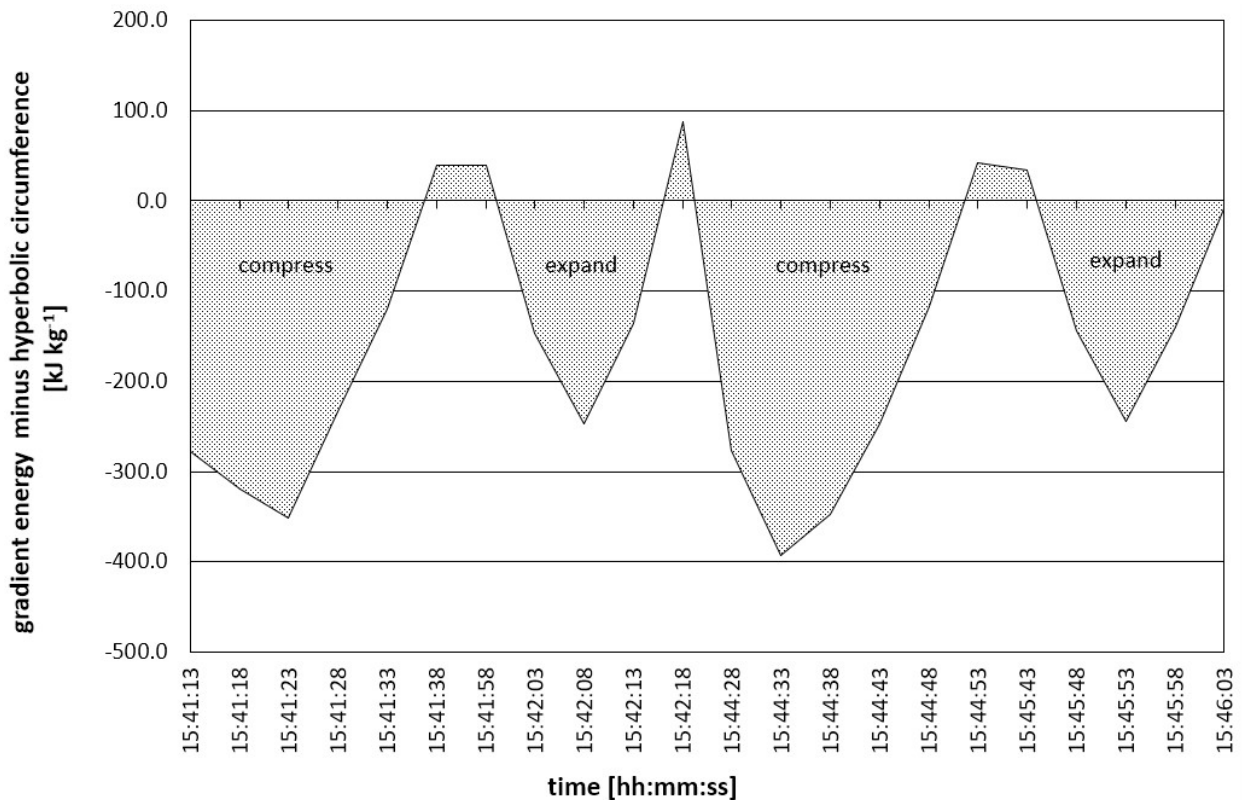


**Fig. 12. Phase transitions with respect to gradient energy and hyperbolic circumference**

Whilst curvature, in the form of hyperbolic circumference, contributes significantly to the gradient energy term, it appears that the inertial reaction of the dissipative structures induces a delay in the response of hyperbolic curvature to the gradient energy potential. The overriding symmetry of the constant Hamiltonian function 'pulls' another, unknown energy source into the system. This bears some similarity to the production of a current-sustaining plasma in a high-voltage electric arc. As the hyperbolic circumference recovers and attains a stable condition, for both the fully contracted and fully expanded piston positions, this additional source of energy diminishes and disappears. At these points the hyperbolic circumference completely satisfies the gradient energy term. It appears that the inertial reaction of the condensed matter system exposes an energy contribution normally suppressed by the instantaneous response of matter to its underlying manifold. This additional source continues to deliver  $P$ - $V$  expansion and contraction work, as it emerges from a second-order phase transition.

For the isochoric case, it seemed reasonable to propose that equal-and-opposite changes in relative permittivity and relative permeability underpin the constant Hamiltonian. Such a relationship becomes evident when combining Einstein's mass-energy equivalence formula with Maxwell's electromagnetic wave equation [1]. With a frustrated 'spin ice' system responsible for a local minimum of energy, the existence of effective monopoles also appears to be a reasonable postulate [3,4,5].

During Stage 1-2, compression of the working fluid produces only a minor increase in density although the curvature of the hyperbolic manifold is seen to reduce with a corresponding reduction in structural inertia of the fluid. To maintain the local energy associated with the lattice of corner-sharing monopoles, relative permeability of the fluid should increase so as to reduce the magnetostatic Coulomb potential. It then follows that a corresponding decrease in relative permittivity occurs, such that the electrostatic Coulomb potential increases. It is possible for such a relationship exists between the effective magnetic monopoles and the electrostatic vdW interaction, as described above. Since effective monopoles can produce effects consistent with inertia and mass [19], such a mechanism appears relevant to the exposition of the experimental results.

Effective monopoles are defects in the texture of the auxiliary magnetic field  $\mathbf{H}$  [19]. During Stage 3-4, the work producing expansion can be partially explained by the curvature/ circumference on the hyperbolic manifold. The magnetic component of the vdW interaction may act as a seed field for the effective lattice-based monopoles which gain in strength until the vdW contribution is exhausted and the value of the  $\mathbf{H}$  field reaches zero. The mechanism is unknown but could be associated with the Zeeman effect [20] or have some cosmological analogue [21]. A phase transition involving the condensation of monopoles into a single quantum state then becomes viable at  $\mathbf{H} = 0$  [22], just as Cooper pairs of electrons coalesce into a Bose-Einstein condensate during formation of a low-energy superconductor [23]. The symmetry-breaking condensation of magnetic monopoles is a corresponding effect that leads to the creation of a dual superconductor phase [8]. In this model, the Meissner effect acts to expel the electric field  $\mathbf{E}$  and gauge invariance of the system is broken, as it is in the superconductor [8]. A quantum state emerges at the point where the curvature of matter detaches from the curvature of the underlying manifold, ie. where the fluid becomes non-relativistic.

It is proposed that dual superconductivity becomes established between the transition points TP1 and TP2 in **Fig. 10** above. Here the system is effectively purged of all short-range and long-range interactions (gravity is insignificant relative to the dissipative structural bonding of the clathrate hydrates) but continues to undergo  $P$ - $V$  expansion in response to the still increasing negative gradient energy term. The only reasonable solutions able to reconcile reducing internal energy with increasing gradient potential appear to be cosmological models involving the false vacuum and emergent geometry [24].

Constant total energy density  $E$  and a repulsive gravitational field from a large negative pressure are defining characteristics of the false vacuum [25]. Corresponding phenomena are evident in the experimental results presented here; constant Hamiltonian and  $P$ - $V$  expansion arising from a negative gradient potential. Then, for the final stage of  $P$ - $V$  expansion, an additional source of energy must be accounted for, a source reminiscent of the cosmological constant [24, 26]. Through the inertial response of its dissipative structures, the system maintains its metastable, sombrero potential with negative energy gradient throughout. Once all short-range and long-range interactions have been effectively eliminated, vacuum energy seems to be the only credible energy source able to flow in response to the gradient potential imposed by the symmetry of the Hamiltonian function [27]. This vacuum energy would enter the system via the condensed monopoles and manifest as the emergent space responsible for the observed expansion work [24].

## Conclusion

Phase transitions that maintain energy conservation in a dissipative system have been described. These low energy transitions take place at a local minimum of energy under negative pressure where complex, dissipative structures within a 'spin ice' lattice maintain a constant Hamiltonian function through structural reorganisation.

Evidence for the constant Hamiltonian, previously described as an analogue of the false vacuum, comes from the non-additivity of thermodynamic potentials within the fundamental thermodynamic relation. The same non-equilibrium relationship is now demonstrated for variable-volume conditions producing mechanical work. The metastable state of the dissipative structures is maintained by a small heat flux flowing into the system from an external heat bath.

During experimental investigations, these second-order phase-changes have been harnessed in the generation of mechanical work. The initial phase transition involves the separation of guest methane molecules from clathrate hydrate hosts to establish a long-range van der Waals (vdW) interaction. The  $-1/r$  relationship is undistorted since the short-range interactions have been neutralised within a dielectric solvent.

Non-extensivity of fluid density with respect to the swept volume of the piston expander reveals a hyperbolic curvature that maps directly to the inertial energy associated with the cylindrical volume. Changes in curvature occur within the constant Hamiltonian such that a reciprocal relationship between relative permeability and relative permittivity is established. This is interpreted as an exchange of energy between the long-range vdW interaction of the inclusion compounds and the effective magnetic monopoles of the frustrated lattice in which they are embedded.

The  $P$ - $V$  work of the piston expander, together with values of internal energy and excess internal energy, reveals a gradient energy term within the Lagrangian function of the system. The complex scalar field potential is a second-order function of  $P$ - $V$  work and comparison provides evidence for a further second-order phase transition. This would be the point at which all the energy of the long-range vdW interaction is transferred to the effective monopoles. Here, the auxiliary magnetic  $\mathbf{H}$  field would reach zero potential and the monopoles would coalesce into a single quantum state to create a dual superconductor.

During this second phase, the gradient energy is no longer fully described by the hyperbolic circumference of the fluid and an additional energy source needs to be accounted for. The local minimum of energy of the constant Hamiltonian is maintained throughout. Since the system is effectively purged of all short-range and long-range interactions, it is proposed that the additional source is vacuum energy flowing in response to the increasing negative energy gradient.

The need to employ relativistic and quantum theories in describing the experimental findings may attract interest from a wide range of investigators, scientists and technologists since the implications are potentially far-reaching. To this end, it is hoped that the experimental results and theories presented here will be the subject of more rigorous mathematical analysis and interpretation.

## References

- [1] M. Gibbons, *J. Phys. Commun.*, **5**, 065005, (2021).
- [2] R. Clausius, *On a Mechanical Theorem Applicable to Heat* (1870), The London, Edinburgh, and Dublin Philosophical Magazine and Journal of Science, **40**, 265, 122-127.
- [3] C. Castelnovo, R. Moessner, and S. L. Sondhi, *Annual Review of Condensed Matter Physics*, **3**, 33-55, (2012).
- [4] C. Castelnovo, R. Moessner, and S. L. Sondhi, *Nature*, **451**, 42-45, (2008).

- [5] R. Arttu, *Phil. Trans. R. Soc. A*, **370**, 5705–5717, (2012).
- [6] S. J. Blundell and K. M. Blundell, *Concepts in Thermal Physics* (Oxford University Press, 2006), Chap. 28.
- [7] P. Coleman, *Introduction to Many-Body Physics* (Cambridge University Press, 2015), Chap. 11
- [8] G. Ripka, *Dual superconductor models of color confinement*, *Lecture Notes in Physics* (2004), Chap. 1,3,5.
- [9] R. B. Peterson, *Energy Sources*, **20**, 3, (1998).
- [10] E. W. Lemmon, L. H. Huber, M.O. McLinden, and I. Bell, *Reference Fluid Thermodynamic and Transport Properties Database (REFPROP)* (Boulder, Colorado, 2020).
- [11] A. Perrin, O. M. Musa, and J. W. Steed, *Chemical Society Reviews*, **5** (2013).
- [12] A. Imre, K. Martinás, and L.P.N. Rebelo, *Thermodynamics of Negative Pressure in Liquids, Non-Equilibrium Thermodynamics*, **23**, 4 (1998).
- [13] B. Lee, *The Journal of Chemical Physics*, **83**, 2421 (1985).
- [14] A. Campa, L. Casetti, I. Latella, A. Pérez-Madrid, and S. Ruffo, *Entropy*, **20**, 12, 907 (2018).
- [15] P. Glansdorff, I. Prigogine, *Thermodynamic Theory of Structure, Stability and Fluctuations* (Wiley-Interscience, London, 1971), Chap. 1, 2.
- [16] V. Kaiser *et al*, *Phys. Rev. B*, **98**, 144413, (2018).
- [17] A-C. Davis and T.W.B. Kibble, *Contemporary Physics*, **46**, 5 (2005).
- [18] R. Moessner, A. P. Ramirez, *Physics Today*, **59**, 2, 4, (2006).
- [19] N. P. Armitage, *Physica B: Condensed Matter*, **536**, 353-358, (2018).
- [20] R. V. Krems, *Phys. Rev. Lett.*, **93**, 013201, (2004)
- [21] B. Ratra, *ApJL*, **391**, L1, (1992)
- [22] J. S. Langer, *Annals of Physics*, **41**, 108-157 (1967)
- [23] J. Bardeen, L. N. Cooper, and J. R. Schrieffer, *Phys. Rev.*, **108**, 1175, (1957).
- [24] A. D. Linde, *Rep. Prog. Phys.*, **47**, 925, (1984)
- [25] A. H. Guth, *Proc. Matl. Acad. Sci. USA*, **90**, 4871-4877, (1993).
- [26] P. J. E. Peebles and B. Ratra, *Rev. Mod. Phys.*, **75**, 559, (2003).
- [27] S. M. Carroll, *Phys. Rev. Lett.*, **81**, 3067, (1998).